

G. A. Ateshian · K. D. Costa · C. T. Hung

A theoretical analysis of water transport through chondrocytes

Received: 24 July 2005 / Accepted: 28 October 2005 / Published online: 17 May 2006
© Springer-Verlag 2006

Abstract Because of the avascular nature of adult cartilage, nutrients and waste products are transported to and from the chondrocytes by diffusion and convection through the extracellular matrix. The convective interstitial fluid flow within and around chondrocytes is poorly understood. This theoretical study demonstrates that the incorporation of a semi-permeable membrane when modeling the chondrocyte leads to the following findings: under mechanical loading of an isolated chondrocyte the intracellular fluid pressure is on the order of tens of Pascals and the transmembrane fluid outflow, on the order of picometers per second, takes several days to subside; consequently, the chondrocyte behaves practically as an incompressible solid whenever the loading duration is on the order of minutes or hours. When embedded in its extracellular matrix (ECM), the chondrocyte response is substantially different. Mechanical loading of the tissue leads to a fluid pressure difference between intracellular and extracellular compartments on the order of tens of kilopascals and the transmembrane outflow, on the order of a nanometer per second, subsides in about 1 h. The volume of the chondrocyte decreases concomitantly with that of the ECM. The interstitial fluid flow in the extracellular matrix is directed around the cell, with peak values on the order of tens of nanometers per second. The viscous fluid shear stress acting on the cell surface is several orders of magnitude smaller than the solid matrix shear stresses resulting from the ECM deformation. These results provide new insight toward our understanding of water transport in chondrocytes.

1 Introduction

Chondrocytes regulate the metabolism of articular cartilage. Because of the avascular nature of adult cartilage, nutrients and waste products are transported to and from the chondrocytes by diffusion and convection through the extracellular matrix (ECM). The convective process is typically driven by mechanical loading of the articular layers, which enhances the flow of interstitial fluid within the tissue (Mauck et al. 2003; O'Hara et al. 1990). This interstitial fluid consists mainly of water, which constitutes between 68 and 85% of the wet weight of adult cartilage (Maroudas 1979; Mow et al. 2005). The transport of interstitial fluid through cartilage has long been established from permeation experiments (Mansour and Mow 1976; Maroudas and Bullough 1968; Stockwell and Barnett 1964) or from measurements of the net loss of tissue weight under prolonged loading (Maroudas et al. 1985). A more detailed examination of fluid flow patterns under various loading configurations has been estimated from theoretical and computational analyses which account for the porous-hydrated nature of cartilage (Ateshian et al. 1994; Ateshian and Wang 1995; Hou et al. 1992; Mow and Mansour 1977; Spilker et al. 1992). Most of these models are concerned with the fluid flow profile within the ECM and do not explicitly incorporate chondrocytes.

It is known from experimental measurements that water transports into and out of chondrocytes, as observed from volume changes resulting from osmotic loading of isolated cells (Guilak 2000; McGann et al. 1988; Xu et al. 2003) or prolonged mechanical compression of cartilage explants (Guilak et al. 1995). It is less clear whether chondrocytes 'attract' interstitial fluid flow streamlines toward them, or 'repel' the streamlines around them. Computational models of the chondrocyte in its pericellular matrix have focused on the deformation, stresses and fluid pressure induced by loading, rather than interstitial fluid flow profiles (Bachrach et al. 1995; Guilak and Mow 2000; Wu et al. 1999; Wu and Herzog 2000). These computational models have described the cell and its ECM as mixtures of a solid matrix, interstitial

G. A. Ateshian (✉) · K. D. Costa · C. T. Hung
Department of Biomedical Engineering, Columbia University,
500 West 120th St. 242 S.W. Mudd,
MC4703 New York, NY 10027, USA
E-mail: ateshian@columbia.edu
Tel.: +1-212-8548602
Fax: +1-212-8543304

G. A. Ateshian
Department of Mechanical Engineering, Columbia University,
New York, NY 10027, USA

fluid, and in some cases, ions, but the semi-permeable nature of the cell membrane has not yet been incorporated in these analyses.

Conversely, investigations of the response of chondrocytes to osmotic loading have modeled the cell as a fluid-filled semi-permeable membrane, yielding measurements of the membrane permeability to water and various osmolytes (McGann et al. 1988; Xu et al. 2003). However, these analyses did not address mechanical loading of chondrocytes, whether isolated or in situ.

The objectives of this theoretical study are twofold. First, the semi-permeable nature of the membrane is incorporated into a refined model of the chondrocyte, to account for its role in regulating water transport into and out of the cell, using membrane permeability values determined from osmotic loading measurements. This model is used to predict the response of the isolated chondrocyte to unconfined compression and these predictions are used to interpret experimental results reported in the recent literature. The associated hypothesis is that the water loss during mechanical loading of chondrocytes is negligible under most testing configurations.

The second objective is to model the cell and its surrounding semi-permeable membrane under in situ loading conditions, embedded within the ECM or within agarose gel. The associated hypothesis is that the interstitial fluid flows around the chondrocyte, not into it, as a result of the lower permeability of its membrane relative to that of the surrounding matrix or gel. These analyses aim to unify the disparate modeling approaches adopted in the literature, where the chondrocyte is variably modeled as a porous-permeable gel with no surrounding membrane, as an incompressible viscoelastic solid, or as a fluid-filled semi-permeable membrane. They also aim to clarify the pattern of water transport in and around chondrocytes.

2 Theoretical framework

Many levels of theoretical refinement are possible when modeling cells. For the purpose of the current analysis, the chondrocyte is modeled as a homogeneous gel, representing the protoplasm (cytoplasm, cytoskeleton, and all enclosed organelles), surrounded by a membrane which is permeable to water and certain solutes, but not to ions. In this treatment, which focuses on mechanical loading of the cell, the protoplasm is modeled as a mixture of a solid matrix and interstitial water. For simplicity, ions and other solutes present inside and outside the cell are not considered, since this study does not specifically address chondrocyte osmotic loading (Ateshian et al. 2006, in press).

The governing equations for the mixture of a solid and a fluid constituent are given by (Mow et al. 1980)

$$\text{div}(\mathbf{v}^s + \mathbf{w}) = 0 \quad (1)$$

$$\mathbf{w} = -k \text{grad} p \quad (2)$$

$$-\text{grad} p + \text{div} \boldsymbol{\sigma}^e = 0 \quad (3)$$

where \mathbf{v}^s is the solid matrix velocity, \mathbf{w} is the volumetric flux of fluid relative to the solid, p is the fluid pressure, $\boldsymbol{\sigma}^e$ is the effective (or elastic) stress, and k is the hydraulic permeability of the solid matrix. The first of these equations is the conservation of mass relation for the mixture; the second is a consequence of the conservation of momentum for the fluid constituent, and reduces to Darcy's law; the last equation is the conservation of momentum for the mixture. For a linear isotropic elastic solid matrix,

$$\boldsymbol{\sigma}^e = \lambda_s (\text{tr} \mathbf{E}) \mathbf{I} + 2\mu_s \mathbf{E} \quad (4)$$

where \mathbf{E} is the infinitesimal strain tensor and λ_s, μ_s are the Lamé constants of the solid matrix. The strain is related to the solid matrix displacement \mathbf{u} through $\mathbf{E} = (\text{grad} \mathbf{u} + \text{grad}^T \mathbf{u})/2$, whereas the solid velocity is given by $\mathbf{v}^s = D^s \mathbf{u} / Dt \approx \partial \mathbf{u} / \partial t$, where D^s / Dt represents the material derivative with respect to the solid matrix.

The equations of mixture theory can easily be reduced to the case of a membrane (Ateshian et al. 2006, in Press). The fluid flux normal to a membrane of unit outward normal \mathbf{n} is given by

$$w_n = \mathbf{w} \cdot \mathbf{n} = -k_m \text{grad} p \cdot \mathbf{n}$$

where k_m is the membrane hydraulic permeability. For a thin membrane of thickness h_m the pressure gradient normal to the membrane is given by

$$-\text{grad} p \cdot \mathbf{n} \approx \frac{\Delta p}{h_m}$$

where $\Delta p = p(x) - p(x + h_m)$ is the upstream-to-downstream pressure difference and x represents the coordinate direction along \mathbf{n} . Thus

$$w_n = L_p \Delta p \quad (5)$$

where

$$L_p \equiv \frac{k_m}{h_m} \quad (6)$$

is the membrane hydraulic conductivity.

3 Unconfined compression of isolated chondrocytes

We now model unconfined compression of a chondrocyte, in analogy to the recent experimental study of Leipzig and Athanasiou (2005). When compressed between two frictionless impermeable loading platens, it is assumed that the cell takes the form of a cylindrical disk surrounded by a semi-permeable membrane (Fig. 1). The membrane is assumed to have negligible tensile stiffness so that the primary contribution to the cell stiffness results from the protoplasm. The fluid flow only occurs in the radial direction, while the axial strain is uniform. For this unconfined compression configuration the dependent variables are $p(r, t)$, $u_r(r, t)$, $\varepsilon_z(t) = \partial u_z / \partial z$, where $\varepsilon_z = E_{zz}$ is the axial normal strain. Thus the governing Eqs. (1)–(4) reduce to

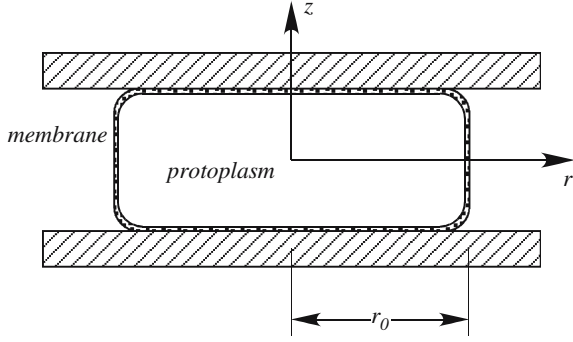


Fig. 1 Unconfined compression of isolated chondrocyte with rigid impermeable frictionless loading platens. Under a sufficiently large tare strain the cell is assumed to take a nearly cylindrical shape. The protoplasm and membrane have different water transport properties

$$\frac{1}{r} \frac{\partial}{\partial r} \left[r \left(\frac{\partial u_r}{\partial t} + w_r \right) \right] + \dot{\varepsilon}_z(t) = 0 \quad (7)$$

$$w_r = -k \frac{\partial p}{\partial r} \quad (8)$$

$$-\frac{\partial p}{\partial r} + H_A \left(\frac{\partial^2 u_r}{\partial r^2} + \frac{1}{r} \frac{\partial u_r}{\partial r} - \frac{u_r}{r^2} \right) = 0 \quad (9)$$

where $H_A = \lambda_s + 2\mu_s$ is the aggregate modulus. Integrating (7) with respect to r and making use of the boundary condition of zero radial displacement along the centerline yields

$$w_r = -\frac{\partial u_r}{\partial t} - \frac{r}{2} \dot{\varepsilon}_z(t). \quad (10)$$

Combining these relations produces the partial differential equation

$$\frac{\partial^2 u_r}{\partial r^2} + \frac{1}{r} \frac{\partial u_r}{\partial r} - \frac{u_r}{r^2} - \frac{1}{H_A k} \frac{\partial u_r}{\partial t} = \frac{1}{H_A k} \frac{r}{2} \dot{\varepsilon}_z(t). \quad (11)$$

The boundary conditions require that the radial displacement reduce to zero at the center,

$$u_r(0, t) = 0, \quad (12)$$

the total normal radial stress at the radial edge r_0 is equal to zero,

$$-p(r_0, t) + \lambda_s \left[\frac{1}{r} \frac{\partial}{\partial r} (r u_r) + \varepsilon_z(t) \right]_{r=r_0} + 2\mu_s \frac{\partial u_r}{\partial r} \Big|_{r=r_0} = 0, \quad (13)$$

and the ambient pressure at the radial edge is zero, which combines with (2) and (5) to yield

$$L_p p(r_0, t) = w_r(r_0, t) = -k \frac{\partial p}{\partial r} \Big|_{r=r_0}. \quad (14)$$

Combining (13) and (14) produces the boundary condition

$$\frac{k}{L_p} \frac{\partial p}{\partial r} \Big|_{r=r_0} + \lambda_s \left[\frac{1}{r} \frac{\partial}{\partial r} (r u_r) + \varepsilon_z(t) \right]_{r=r_0} + 2\mu_s \frac{\partial u_r}{\partial r} \Big|_{r=r_0} = 0 \quad (15)$$

We can consider two limiting cases which simplify the analysis of this problem. In the first case, we can assume that the membrane permeability is much greater than the protoplasm permeability, which implies that the membrane offers negligible resistance to fluid flow compared to the protoplasm. This is equivalent to letting $r_0 L_p / k \gg 1$ in (15), which yields the governing equations for unconfined compression of a biphasic disk, the solution of which is given by Armstrong et al. (1984). Leipzig and Athanasiou (2005) have shown that this type of model does not yield a good fit of the experimental response of chondrocytes to unconfined compression creep, which concurs with our intuitive physical perspective (and the established dogma in cell biophysics) that this limiting case is not realistic.

The second case considers the opposite limit where we assume that the resistance to fluid flow across the membrane is much greater than in the protoplasm, $r_0 L_p / k \ll 1$. Then, multiplying (11) with $r_0 L_p$ and neglecting terms with the coefficient $r_0 L_p / k$, we get

$$\frac{\partial^2 u_r}{\partial r^2} + \frac{1}{r} \frac{\partial u_r}{\partial r} - \frac{u_r}{r^2} = \frac{\partial}{\partial r} \left[\frac{1}{r} \frac{\partial}{\partial r} (r u_r) \right] = 0.$$

The solution to this ordinary differential equation is

$$u_r = \varepsilon_r(t) r \quad (16)$$

where $\varepsilon_r = E_{rr}$ is the radial normal strain. This shows that, under this limiting condition, the radial normal strain in the protoplasm is uniform. Substituting this result into (9) shows that the pressure is also uniform, $p = p(t)$. Combining (10), (13), (14) and (16) yields

$$\tau_\varepsilon \left[\dot{\varepsilon}_r(t) + \frac{1}{2} \dot{\varepsilon}_z(t) \right] + \varepsilon_r(t) + \nu \varepsilon_z(t) = 0 \quad (17)$$

where

$$\tau_\varepsilon \equiv \frac{(1-\nu)r_0}{H_A L_p} \quad (18)$$

and ν is Poisson's ratio of the solid matrix of the protoplasm, related to λ_s and μ_s via $\lambda_s = 2\mu_s \nu / (1-2\nu)$.

The axial normal stress $\sigma_z(t)$ acting on the loading platens is given by

$$\frac{\sigma_z(t)}{H_A} = -\frac{p(t)}{H_A} + \frac{2\nu}{1-\nu} \varepsilon_r(t) + \varepsilon_z(t).$$

To get the pressure, we use (13) which yields

$$\frac{p(t)}{H_A} = \frac{\varepsilon_r(t) + \nu \varepsilon_z(t)}{1-\nu} \quad (19)$$

so that

$$\frac{\sigma_z(t)}{H_A} = \frac{1-2\nu}{1-\nu} [\varepsilon_z(t) - \varepsilon_r(t)]. \quad (20)$$

These equations can be solved for $\sigma_z(t)$ given $\varepsilon_z(t)$ (stress-relaxation problem), or for $\varepsilon_z(t)$ given $\sigma_z(t)$ (creep problem), as shown next.

3.1 Stress-relaxation

For stress-relaxation in response to a step strain of magnitude ε_0 , where $\varepsilon_z(t) = \varepsilon_0 H(t)$, (17) reduces to

$$\tau_\varepsilon \dot{\varepsilon}_r(t) + \varepsilon_r(t) + \nu \varepsilon_0 = 0. \quad (21)$$

The solution to this equation, subject to the initial condition that the instantaneous volume change is zero, $2\varepsilon_r(0^+) + \varepsilon_z(0^+) = 2\varepsilon_r(0^+) + \varepsilon_0 = 0$, is

$$\varepsilon_r(t) = - \left[\nu + \frac{(1-2\nu)}{2} e^{-t/\tau_\varepsilon} \right] \varepsilon_0. \quad (22)$$

The axial stress (20) is then given by

$$\begin{aligned} \frac{\sigma_z(t)}{E_Y} &= \left[1 + \frac{(1-2\nu)}{2(1+\nu)} e^{-t/\tau_\varepsilon} \right] \varepsilon_0 \\ &= \left[1 - \left(1 - \frac{\tau_\sigma}{\tau_\varepsilon} \right) e^{-t/\tau_\varepsilon} \right] \varepsilon_0 \end{aligned} \quad (23)$$

where Young's modulus E_Y is related to the aggregate modulus via

$$E_Y = \frac{(1+\nu)(1-2\nu)}{1-\nu} H_A \quad (24)$$

and τ_σ is given in (31) below. The dilatation (relative change in volume) is given by

$$e(t) = 2\varepsilon_r(t) + \varepsilon_z(t) = (1-2\nu) (1 - e^{-t/\tau_\varepsilon}) \varepsilon_0 \quad (25)$$

and the fluid pressure inside the cell can be determined from (19) and (22),

$$p(t) = - \frac{E_Y}{2(1+\nu)} \varepsilon_0 e^{-t/\tau_\varepsilon} = -\mu_s \varepsilon_0 e^{-t/\tau_\varepsilon}. \quad (26)$$

3.2 Creep

For creep in response to $\sigma_z(t) = \sigma_0 H(t)$, (20) yields

$$\varepsilon_z(t) = \frac{1-\nu}{1-2\nu} \frac{\sigma_0}{H_A} + \varepsilon_r(t) \quad (27)$$

which when substituted into (17) produces

$$\frac{3}{2} \tau_\varepsilon \dot{\varepsilon}_r(t) + (1+\nu) \varepsilon_r(t) + \frac{\nu(1-\nu)}{1-2\nu} \frac{\sigma_0}{H_A} = 0. \quad (28)$$

This ordinary differential equation needs to be solved subject to the initial condition

$$2\varepsilon_r(0^+) + \varepsilon_z(0^+) = 3\varepsilon_r(0^+) + \frac{1-\nu}{1-2\nu} \frac{\sigma_0}{H_A} = 0. \quad (29)$$

The solution is given by

$$\varepsilon_r(t) = - \left(\nu + \frac{1-2\nu}{3} e^{-t/\tau_\sigma} \right) \frac{\sigma_0}{E_Y} \quad (30)$$

where

$$\tau_\sigma \equiv \frac{3\tau_\varepsilon}{2(1+\nu)} = \frac{3r_0(1-2\nu)}{2E_Y L_p}. \quad (31)$$

Substituting this result into (27) yields

$$\begin{aligned} \varepsilon_z(t) &= \left(1 - \frac{1-2\nu}{3} e^{-t/\tau_\sigma} \right) \frac{\sigma_0}{E_Y} \\ &= \left[1 - \left(1 - \frac{\tau_\varepsilon}{\tau_\sigma} \right) e^{-t/\tau_\sigma} \right] \frac{\sigma_0}{E_Y}. \end{aligned} \quad (32)$$

and the dilatation is

$$e(t) = 2\varepsilon_r(t) + \varepsilon_z(t) = (1-2\nu) (1 - e^{-t/\tau_\sigma}) \frac{\sigma_0}{E_Y} \quad (33)$$

The fluid pressure inside the cell is determined from (19), (30) and (32),

$$p(t) = - \frac{\sigma_0}{3} e^{-t/\tau_\sigma} \quad (34)$$

3.3 Analysis of response

When modeled as a fluid–solid mixture surrounded by a semi-permeable membrane, the response of a chondrocyte to unconfined compression stress-relaxation or creep follows an exponential profile of the same mathematical form as for a standard linear solid (Kelvin model), where the time constant is given by either τ_ε in (18) or τ_σ in (31). The equilibrium response ($t \rightarrow \infty$) for either loading profile is the same according to (23) and (32), obeying $\sigma_z(\infty) = E_Y \varepsilon_z(\infty)$. Experimentally, Young's modulus of chondrocytes has been determined from either micropipette aspiration (Guilak et al. 1999; Jones et al. 1999), unconfined compression (Leipzig and Athanasiou 2005), indentation with atomic force microscopy (Hung et al. 2001), or compression of cell-seeded agarose constructs (Freeman et al. 1994), yielding consistent results where E_Y is on the order of 1 kPa.

The determination of Poisson's ratio is more problematic in light of the implications of the results of this analysis, as elaborated below. In porous media theories, Poisson's ratio may be determined either before fluid has drained from the medium ('instantaneous' Poisson's ratio), or after it has drained ('equilibrium' Poisson's ratio). In most porous media models of soft biological tissues (including the current analysis), the fluid and solid are assumed to be intrinsically incompressible, yielding an instantaneous Poisson's ratio of 0.5. The equilibrium Poisson's ratio, ν , is generally less than 0.5. In fact, if $\nu = 0.5$, the implication is that there is no fluid flow in the porous medium under any loading condition, for example as in the case of non-communicating closed pores. (This is confirmed by the results of (25) and (33) which yield $e(t) = 0$ when $\nu = 0.5$.) For chondrocytes, ν has been estimated from experimental measurements to be 0.4 by Freeman et al. (1994) who compressed chondrocytes embedded in agarose gels, and 0.26 by Shieh and Athanasiou (2005, in press) who performed unconfined compression of isolated cells. More recently, Trickey et al. (2006, in press) have reported a value of 0.37, estimated from micropipette aspiration and release experiments.

To estimate the time constants τ_ε and τ_σ , we require measures of the membrane hydraulic conductivity. From osmotic loading experiments on chondrocytes, McGann et al.

(1988) and Xu et al. (2003) reported values of L_p on the order of $3 \times 10^{-14} \text{ m}^3/\text{N s}$ at room temperature. Substituting $E_Y \sim 1 \text{ kPa}$, $\nu \sim 0.33$, $L_p \sim 3 \times 10^{-14} \text{ m}^3/\text{N s}$ and $r_0 \sim 10 \mu\text{m}$ into (18) and (31), and using (24) yields $\tau_\varepsilon \sim 42 \text{ h}$ and $\tau_\sigma \sim 47 \text{ h}$. Smaller values of Poisson's ratio yield even larger time constants since the relative volume loss at equilibrium is larger (Fig. 2a), requiring longer time for fluid to escape; for example, for $\nu \sim 0$, the time constants are $\tau_\varepsilon \sim 93 \text{ h}$ and $\tau_\sigma \sim 139 \text{ h}$. (From (18) and (31), it can also be deduced that larger cell sizes, smaller equilibrium compressive moduli and smaller membrane conductivities would also increase the time constants for reaching equilibrium.) These are surprisingly elevated time constants, considering that the time constant for chondrocyte volume change under osmotic loading is more typically on the order of seconds or minutes (McGann et al. 1988; Xu et al. 2003). For compressive strains ε_0 of magnitude $\sim 10\%$, the peak intracellular fluid pressure can be estimated from (26) to range from ~ 40 to 50 Pa (Fig. 2b). The peak transmembrane fluid flux can be determined by substituting this value into (5), with the extracellular pressure equal to zero (ambient conditions) to yield $w_n \sim 1.2 - 1.5 \text{ pm/s}$.

The obvious implication from this result is that there is very little fluid flow out of an isolated chondrocyte under mechanical loading conditions where the loading duration is on the order of tens of minutes or even a few hours, since the time constant for significant change in cell volume is on the order of days. Consequently, despite the fact that the cell model allows for fluid flow across the membrane, these results imply that the isolated chondrocyte behaves in practice as an incompressible solid, under purely mechanical loading. Thus, Poisson's ratio measured from mechanical loading of isolated chondrocytes in experiments which last tens of minutes or less is expected to be close to 0.5, even if the true equilibrium Poisson's ratio is significantly smaller.

4 Compression of in situ chondrocytes

To investigate water transport and the volume change of chondrocytes in situ, we perform a finite element analysis conceptually similar to the study of Guilak and Mow (2000). A multiscale analysis is performed whereby the chondrocyte is considered to be embedded within a cylindrical disk of either cartilage or agarose, which is loaded in confined compression creep, with a porous indenter loading the top surface (Fig. 3). The creep response of the whole disk is obtained from the analytical solution of the biphasic theory. The resulting solutions for the displacement and pressure (Mow et al. 1980) are applied as boundary conditions on a finite element mesh of the chondrocyte and its surrounding ECM:

$$u_r(r, z, t) = 0 \quad (35)$$

$$\frac{u_z(r, z, t)}{h} = \left\{ \frac{z}{h} + \frac{2}{\pi^2} \sum_{n=1}^{\infty} (-1)^n \frac{\sin(n - (1/2))\pi(z/h)}{(n - (1/2))^2} \right. \\ \left. \times \exp \left[- \left(n - \frac{1}{2} \right)^2 \pi^2 \frac{H_A k}{h^2} t \right] \right\} \frac{\sigma_0}{H_A} \quad (36)$$

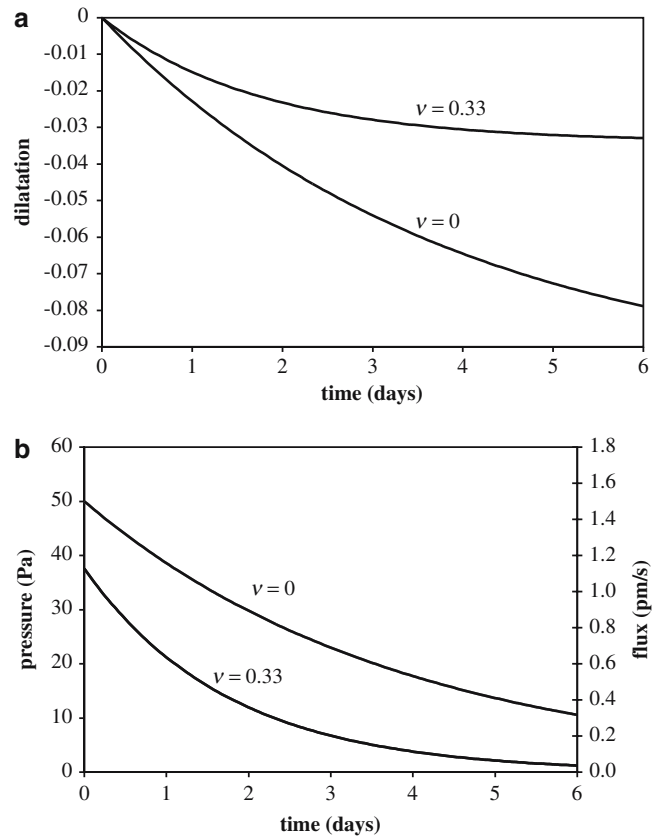


Fig. 2 **a** Cell dilatation (relative change in volume) in the unconfined compression stress-relaxation response of a chondrocyte. $E_Y = 1 \text{ kPa}$, $\nu = 0$ or 0.33 , $L_p = 3 \times 10^{-14} \text{ m}^3/\text{N s}$, $r_0 = 10 \mu\text{m}$, $\varepsilon_0 = -0.10$. **b** Intracellular fluid pressure and transmembrane fluid flux for the same conditions. The fluid flux is proportional to the pressure according to Eq. (5)

$$\frac{p(r, z, t)}{H_A} = \frac{2}{\pi} \sum_{n=1}^{\infty} (-1)^n \frac{\cos(n - (1/2))\pi(z/h)}{n - (1/2)} \\ \times \exp \left[- \left(n - \frac{1}{2} \right)^2 \pi^2 \frac{H_A k}{h^2} t \right] \frac{\sigma_0}{H_A} \quad (37)$$

where h is the disk thickness and σ_0 is the applied axial stress.

4.1 Finite element model

The ECM is modeled as a biphasic disk with $E_Y = 0.64 \text{ MPa}$, $\nu = 0$, and $k = 0.6 \times 10^{-15} \text{ m}^4/\text{N s}$ for cartilage (Soltz and Ateshian 2000), and $E_Y = 10 \text{ kPa}$, $\nu = 0$, and $k = 10^{-13} \text{ m}^4/\text{N s}$ for 2% agarose (Andarawis et al. 2001; Mauck et al. 2000). The thickness is $h = 1 \text{ mm}$ and the chondrocyte is taken to be halfway through the thickness of the disk, $z = h/2$. A constant compressive stress is applied on the tissue via the porous indenter, of magnitude $\sigma_0 = 64 \text{ kPa}$ for cartilage and $\sigma_0 = 1 \text{ kPa}$ for agarose.

The cell is modeled as a biphasic protoplasm surrounded by a semi-permeable membrane, as described above, with

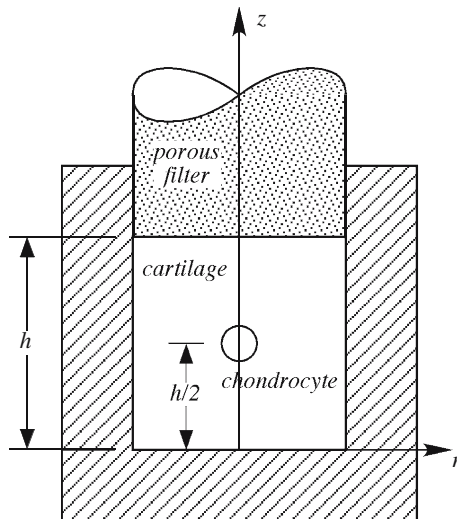


Fig. 3 Confined compression of a cylindrical disk of cartilage. The finite element analysis considers a chondrocyte located halfway through the thickness of the disk

$E_Y = 1 \text{ kPa}$, $\nu = 0.33$, and $k = k_{\text{ECM}}$ for the protoplasm, and $E_Y = E_{Y,\text{ECM}}$, $\nu = \nu_{\text{ECM}}$, and $L_p = 3 \times 10^{-14} \text{ m}^3/\text{N}\cdot\text{s}$ for the membrane. The chondrocyte radius is $r_0 = 10 \mu\text{m}$ and the local ECM region modeled around the cell extends $50 \mu\text{m}$ along the radial direction and $50 \mu\text{m}$ above and below the cell along the axial direction. Because of numerical stability considerations, the true thickness of the membrane (on the order of 10 nm) cannot be modeled. Instead, a layer of thin elements ($h_m = 0.1 \mu\text{m}$) is used to represent the membrane and the hydraulic permeability k_m of these elements is set such that it satisfies Eq. (6) for the desired value of L_p ($k_m = 3 \times 10^{-21} \text{ m}^4/\text{N}\cdot\text{s}$). The validity of this approach was investigated by creating a similar finite element analysis for unconfined compression stress-relaxation of an isolated cell and the solution was verified to follow the theoretical prediction of (22) and (23).

The axisymmetric finite element mesh consists of eight-node isoparametric quadrilateral elements, with 3,052 nodes and 983 elements, created using commercial software (I-deas NX Series v.11, UGS Corp., Plano, TX, USA). The analysis is performed using a custom-written finite element code for biphasic problems (Krishnan et al. 2003) which employs a displacement–pressure (u – p) formulation (Almeida and Spilker 1997; Wayne et al. 1991). Results are plotted using commercial software (Tecplot 10.0, Tecplot Inc., Bellevue, WA, USA).

4.2 Analysis of response

4.2.1 Chondrocytes in Cartilage

Upon loading the average fluid pressure in the chondrocyte is found to exceed the pressure in the surrounding ECM after the initial load application (Fig. 4a). The peak intracellu-

lar and extracellular fluid pressure are initially equal to the applied stress, 64 kPa , producing an initial pressure difference of zero. As time progresses the pressure differential increases to a peak value of $\sim 11.5 \text{ kPa}$ before returning to zero within approximately 1 h (Fig. 4b). As a result of this hyper-pressurization water leaves the chondrocyte at a rate directly proportional to this pressure difference as predicated by Eq. (5). The chondrocyte volume concomitantly decreases with time along with that of the ECM; interestingly, the chondrocyte dilatation is greater in magnitude than the ECM dilatation at equilibrium (Fig. 5).

The water flux w_n out of the chondrocyte achieves a peak velocity of $\sim 0.34 \text{ nm/s}$ (Fig. 4b). This magnitude is considerably smaller than that of the water flux in the ECM, which achieves peak velocities of 50 nm/s . A plot of the flux vectors demonstrates that the flow of interstitial fluid goes predominantly around the chondrocyte (Fig. 6).

When compared with the results of the previous section, these findings demonstrate that mechanical loading of chondrocytes in situ can lead to volume changes at a much higher rate than for isolated chondrocytes (on the order of 1 h in situ versus 2 days ex situ). The primary explanation is that the pressure difference between inside and outside the cell is much greater for in situ than isolated chondrocytes ($\sim 11.5 \text{ kPa}$ in situ versus $\sim 0.04 \text{ kPa}$ ex situ), which causes a much greater water flux out of the cell according to (5). Nevertheless, in situ, most of the water transport in cartilage occurs in the ECM, around the chondrocyte, and not across the chondrocyte membrane.

4.2.2 Chondrocytes in Agarose

When embedded in agarose, the intracellular pressure of the chondrocyte remains elevated for the entire 3,600 s duration of the analysis, whereas the surrounding agarose interstitial fluid pressure decreases toward zero (Fig. 7a). The corresponding pressure difference rises to 900 Pa , producing a peak transmembrane fluid flux of $\sim 27 \text{ pm/s}$, before starting to decrease (Fig. 7b). The decrease in cell volume is significantly slower than the surrounding agarose, with a negative dilatation (relative volume reduction) of 2.4% for the chondrocyte and 8.5% for the agarose, at 3,600 s (Fig. 8). These results suggest that chondrocytes embedded in agarose behave as nearly incompressible inclusions when experiments are conducted in the time frame of minutes, but begin to exhibit measurable volume changes over the time frame of 1 h, albeit less significant than in cartilage ECM.

5 Discussion

The primary objective of this study was to incorporate the role of the cell membrane in the study of water transport in the chondrocyte under mechanical loading. Two loading configurations were used to investigate the mechanical response of isolated chondrocytes and in situ chondrocytes, which are

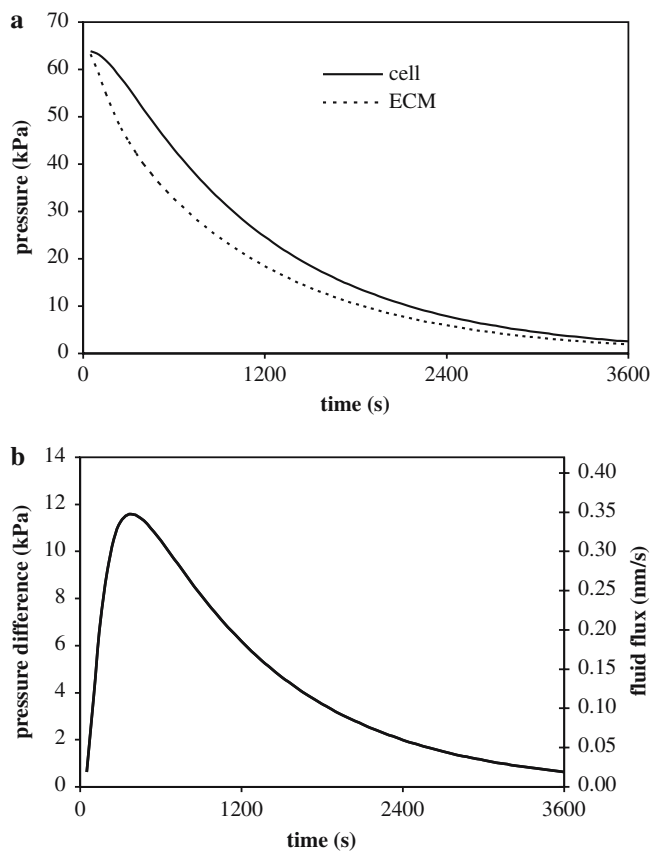


Fig. 4 **a** Intracellular and pericellular average fluid pressure from the finite element analysis of a chondrocyte embedded within its extracellular matrix (ECM). **b** Average fluid pressure difference (cell – ECM) and average transmembrane fluid flux [proportional to the pressure difference according to Eq. (5)]

representative of experimental and theoretical analyses reported in the prior literature. To the best of our knowledge, the role of the membrane in restricting fluid flow into or out of the mechanically loaded chondrocyte has not been previously investigated.

The analysis of unconfined compression of an isolated chondrocyte demonstrates that the magnitude of the fluid pressure inside the cell is a fraction of the equilibrium modulus of the protoplasm, on the order of 40 Pa. Consequently the transmembrane fluid flux, which is proportional to the difference between intracellular and extracellular pressure, is very small (~ 1.2 pm/s). The loss of fluid from the cell takes up to 6 days (Fig. 2) and for all practical purposes the chondrocyte exhibits negligible volume loss and behaves as an incompressible solid. Analyzing the temporal creep response over a shorter period, comparable to the 50 s duration of unconfined testing of chondrocytes in the study of Leipzig and Athanasiou (2005), shows that the present model predicts an elastic-like response, with undetectable temporal variation. Yet, the experiments of Leipzig and Athanasiou show that the creep deformation rises to an equilibrium-like value with a time constant of 3.2 s. Based on the prediction of the current study that fluid flow is negligible over such a short period of time, the transient response measured by Leipzig

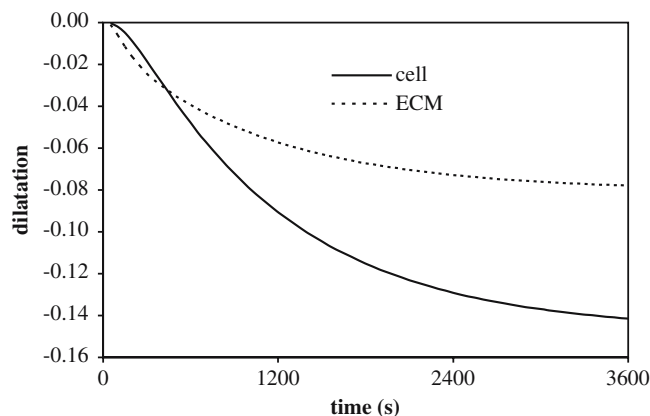


Fig. 5 Intracellular and pericellular average dilatation from the finite element analysis of a chondrocyte embedded within its ECM

and Athanasiou can be attributed to intrinsic viscoelasticity of the solid matrix of the protoplasm. Indeed, these authors found that they could predict the unconfined compression creep response of chondrocytes successfully with a standard solid (Kelvin) model. This observation suggests that a refinement to the model of the chondrocyte adopted in the current study would be to model the protoplasm as a solid–fluid mixture where the solid is intrinsically viscoelastic (Trickey et al. 2006, in Press), surrounded by a semi-permeable membrane.

The analysis of unconfined compression of isolated chondrocytes can also be extended to infer the cell response to micropipette aspiration. In a typical experiment, the pressure difference applied on a chondrocyte during micropipette aspiration is on the order of 0.5 kPa (Jones et al. 1999). According to Eq. (5), using the representative value of L_p adopted throughout this analysis, the predicted transmembrane fluid flux is $w_n \sim 15$ pm/s. For a typical micropipette internal diameter of $9 \mu\text{m}$ (cross-sectional area of $64 \mu\text{m}^2$) and a cell diameter of $20 \mu\text{m}$ (volume of $4,189 \mu\text{m}^3$), the total volume of water aspirated from inside the cell over a typical experimental duration of 600 s is $\text{flux} \times \text{area} \times \text{time} = 0.6 \mu\text{m}^3$, or less than 0.02% of the original cell volume. Consequently, it is expected from this analysis that the chondrocyte should exhibit negligible volume loss and behave as an incompressible solid during micropipette aspiration, as indeed has been assumed in some studies (Haider and Guilak 2000). The time-dependent response of the aspiration length into the micropipette, which has a characteristic time constant of ~ 70 s in chondrocytes (Jones et al. 1999; Trickey et al. 2004), would thus be attributed to intrinsic viscoelasticity of the solid matrix of the protoplasm.

However, this prediction that the chondrocyte volume remains essentially constant during micropipette aspiration is not supported by the experimental results of Jones et al. (1999). In experiments where the entire chondrocyte was aspirated into a micropipette, these authors have reported that the aspiration induces an instantaneous change in chondrocyte volume. For chondrocytes from healthy cartilage, they reported a volume reduction from $1,699 \mu\text{m}^3$ prior to

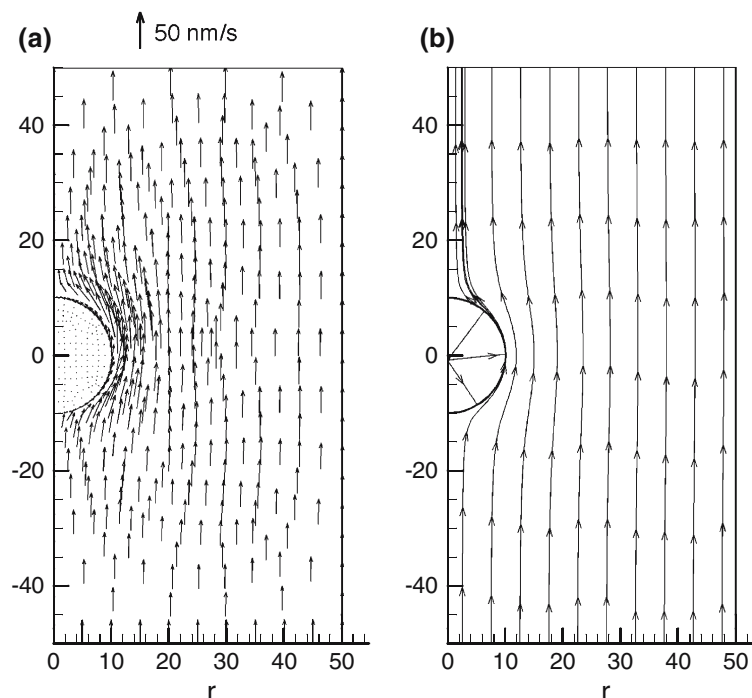


Fig. 6 Fluid flux in the finite element analysis of a chondrocyte embedded within its ECM, evaluated at $t = 300$ s: **a** flux vectors, showing magnitude and direction; **b** streamlines

aspiration down to $1,507 \mu\text{m}^3$ immediately after aspiration; when measured 600 s later, the volume was maintained at $1,503 \mu\text{m}^3$. These types of measurements form the basis for reporting a Poisson's ratio of ~ 0.37 in the recent study of Trickey et al. (2006, in Press).

Based on our analysis, the nearly-instantaneous change in volume reported by Jones et al. cannot be attributed to water loss from the chondrocyte, because of the low permeability of the cell membrane. In fact, the absence of cell volume change observed over 600 s supports the premise of the current analysis that there is negligible water transport out of the cell over such relatively short durations. In contrast, Trickey et al. (2006, in Press) propose that the nearly-instantaneous change in chondrocyte volume upon aspiration can be attributed to water outflow based on modeling the cell as a biphasic gel (with no membrane). At this time, it is difficult to reconcile these contradictory conclusions.

We are thus reduced to consider two other potential explanations for this instantaneous volume change, neither of which can be verified at this time: (1) the solid matrix of the protoplasm is intrinsically compressible, contrary to the modeling assumption adopted in the current analysis (or that of Trickey et al.); this implies that the instantaneous Poisson's ratio can be less than 0.5. While this explanation is theoretically tenable, it predicates a behavior at the cellular level which is not observed at the tissue level. From macroscopic measurements, the solid matrix of cartilage has been shown to be intrinsically incompressible under pressures as high as 12 MPa (Bachrach et al. 1998); osteoblast-like cells have also been shown to be intrinsically incompressible under hydro-

static pressurization (Wilkes and Athanasiou 1996) and it seems unlikely that intracellular components of chondrocytes should behave differently. (2) The inherent uncertainty in the measurement of cell volume may yield potentially large uncertainties in the experimental measurement of Poisson's ratio. Using a straightforward error propagation analysis, the uncertainty in the measurement of the volume $V = 4\pi r_0^3/3$ of a sphere is $\Delta V = 4\pi r_0^2 \Delta r_0$. If the measurement uncertainty for the radius is $\Delta r_0 \sim 0.2 \mu\text{m}$ (the resolution reported by Trickey et al.), this translates into a volume uncertainty of $\Delta V = 138 \mu\text{m}^3$ when $V = 1,699 \mu\text{m}^3$ ($r_0 = 7.4 \mu\text{m}$), or $\Delta V/V = 8\%$. This uncertainty is only slightly smaller than the volume difference observed by Jones et al. (1999) before and after cell aspiration ($1,699 - 1,507 = 192 \mu\text{m}^3$). If the uncertainty in the measurement of r_0 is further compounded by systematic differences resulting from the segmentation algorithm used to identify the cell boundary outside the micropipette, versus using the micropipette diameter for estimating the cell volume after aspiration, as done by Trickey et al., it is possible that the near-instantaneous change in volume observed upon aspiration represents a bias error resulting from the distinct measurement methodologies. We have no evidence to suggest that the methodology of Jones et al. (1999) or Trickey et al. (2006, in Press) introduced such systematic errors; the purpose of this statement is to indicate that the measurement of cell volume inside and outside the micropipette may be subject to certain assumptions and uncertainties. In our opinion, the lack of an observable transient response in the volume of the chondrocyte after it has been aspirated into the micropipette represents a hint that the

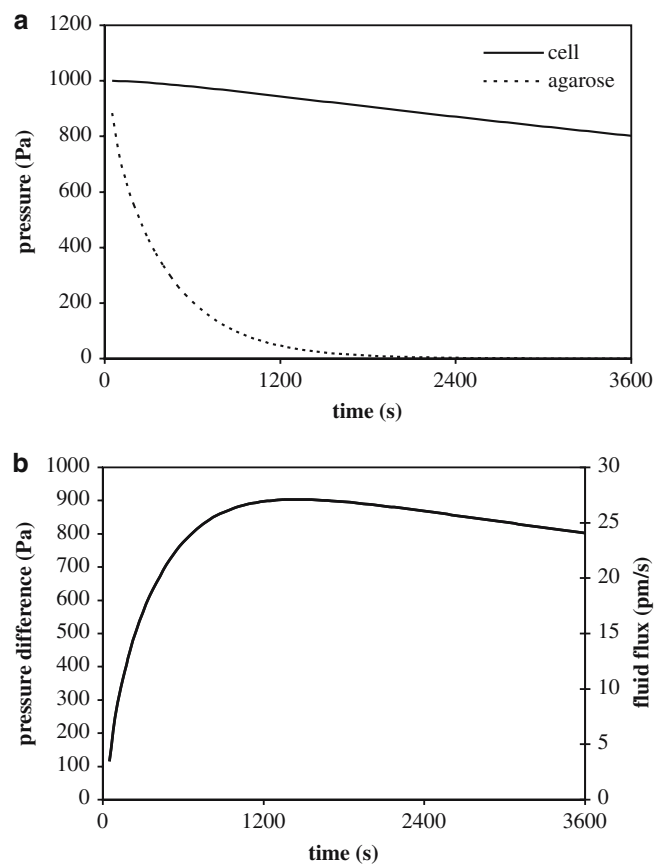


Fig. 7 **a** Intracellular and pericellular average fluid pressure from the finite element analysis of a chondrocyte embedded within an agarose gel. **b** Average fluid pressure difference (cell – agarose) and average transmembrane fluid flux [proportional to the pressure difference according to Eq. (5)]

reported instantaneous volume change cannot be attributed to water outflow.

In the second analysis of this study, it was found that the transmembrane transport of water for an in situ chondrocyte is much more significant than for an isolated chondrocyte. The reason is that the pressure across the cell membrane is on the order of 10^4 Pa under in situ loading, because of the low permeability of the cell membrane relative to the ECM. The resulting relatively large transmembrane flux produces a significant reduction in the chondrocyte volume over a time scale on the order of 1 h (Fig. 5), and it is no longer possible to consider that the chondrocyte behaves as an incompressible viscoelastic solid under in situ conditions. The concomitant change in cell and ECM volume is consistent with the experimental measurements of Guilak et al. (1995) who reported in situ chondrocyte volume changes under equilibrium unconfined compression, using confocal microscopy. In their study, Guilak et al. found that a 15% axial compression of the tissue produced an 18% reduction in cell volume, on average through the depth. In the current computational analysis, a 10% axial compression of the tissue produced a 14% reduction in cell volume, suggesting a consistent outcome between these two studies. The theoretical analyses of Bachrach et al.

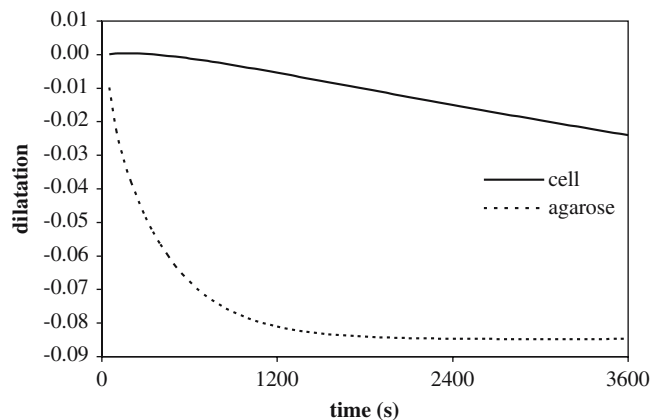


Fig. 8 Intracellular and pericellular average dilatation from the finite element analysis of a chondrocyte embedded within agarose

(1995) and Wu et al. (1999), who modeled the cell and its ECM as biphasic materials, reported similar predictions for the cases where the modulus of the chondrocyte was equal to or smaller than that of the ECM.

The prediction that the intracellular pressure is significantly higher than the extracellular pressure (Fig. 4) was also noted in the theoretical analyses of Bachrach et al. (1995) and Wu et al. (1999), because their model, though not including a cell membrane, assumed a permeability inside the cell one to three orders of magnitude smaller than in the ECM. In contrast, the experimental study of Shin and Athanasiou (1999) on osteoblast-like cells and the study of Leipzig and Athanasiou (2005) on chondrocytes, estimated the biphasic hydraulic permeability of these cells to be three to five orders of magnitude larger than that of the ECM, whereas Trickey et al. (2000) estimated it to be on the same order of magnitude as that of the ECM. As discussed by these authors (Leipzig and Athanasiou 2005; Trickey et al. 2000), these elevated values for cell protoplasm permeability are necessary for predicting the relatively short time constant (on the order of tens of seconds) observed under mechanical loading of isolated cells (including cytoindentation, unconfined compression and micropipette aspiration). Yet, these authors have found that their experimental data are better fitted by a standard viscoelastic Kelvin model, which implies that the observed transient behavior can be better predicted by intrinsic viscoelasticity of the protoplasm, rather than flow-dependent viscoelasticity – which is the interpretation that we also favor.

The results of the finite element analysis demonstrate that the interstitial fluid flux deflects around the chondrocyte instead of flowing into it, with a peak velocity on the order of 50 nm/s tangential to the cell membrane (Fig. 6). This observation raises the intriguing question of whether interstitial fluid flow around the chondrocyte generates a significant viscous shear stress which may influence the cell mechanobiology (Hung et al. 2000; Smith et al. 2000). The biphasic model adopted in our analysis does not explicitly incorporate the viscosity of the interstitial fluid; thus, the shear stress in the fluid cannot be determined from the finite element solution.

However, a straightforward derivation akin to that presented by Hou et al. (1989), where the interstitial fluid viscosity μ_f is incorporated into the constitutive formulation, shows that the fluid shear stress at the cell membrane is given by $\tau = w_\infty \sqrt{\mu_f/k}$. In this expression, w_∞ is the flux outside of the boundary layer resulting from the viscosity of the interstitial fluid; in our analysis, it represents the flux tangential to the cell membrane as determined from the finite element analysis. With $w_\infty = 50$ nm/s and $\mu_f = 1$ mPa.s (the viscosity of water), and using the same value for the ECM permeability k as in the finite element analysis, the peak fluid shear stress is $\tau = 0.065$ Pa. In contrast, the shear stress in the pericellular matrix resulting from the tissue deformation has a peak value of 55 kPa according to the finite element results. This very large difference emphasizes that fluid shear stresses resulting from interstitial fluid flow around chondrocytes are entirely negligible compared to the solid matrix shear stresses resulting from the deformation.

The analysis of a chondrocyte embedded in agarose gel was performed to investigate an experimental model frequently reported in the literature, either for the measurement of chondrocyte deformation (Freeman et al. 1994; Lee and Bader 1995) or for the study of cartilage matrix elaboration and tissue engineering (Buschmann et al. 1992; Mauck et al. 2000). Results show that the chondrocyte volume reduction inside agarose falls in between the two extreme cases of isolated and in situ chondrocytes. The small relative change in volume observed in the current analysis is qualitatively consistent with the estimation of a nearly-incompressible Poisson ratio of 0.4 by Freeman et al. (1994) at the completion of their 15 min test.

A potential limitation of this study is that the finite element mesh did not reproduce the actual thickness of the cell membrane, due to the 1,000 fold difference between cell size (~ 10 μ m) and membrane thickness (~ 10 nm). The actual membrane thickness modeled in the finite element analysis was 100 nm and the value of the membrane permeability was adjusted to yield resistance to transmembrane fluid flux equivalent to the true membrane thickness. To address this potential limitation, a finite element analysis of unconfined compression of an isolated cell was performed using the same modeling assumptions for the cell membrane, and the solution was found to be essentially identical to the theoretical analysis presented in the first part of this study. Therefore, we feel confident that our finite element modeling approach for the cell membrane does not adversely effect the conclusions of this study.

Finally, it should be noted that the analysis of the chondrocyte in situ did not account for the effects of osmotic loading resulting from the increased proteoglycan fixed-charge density with increasing ECM dilatation. Clearly, the concomitant increase in the osmolarity of dissolved ions would produce an additional driving force for the loss of water from the cell. This mechanism may be investigated in future studies by taking into account the role of ions and proteoglycan fixed-charge density.

In summary, this study demonstrates that the incorporation of a semi-permeable membrane when modeling the chondrocyte leads to the following conclusions: under mechanical loading of the isolated chondrocyte, the intracellular fluid pressure is on the order of tens of Pascals and the transmembrane fluid outflow, on the order of picometers per second, takes several days to subside; consequently, the chondrocyte behaves practically as an incompressible solid whenever the loading duration is on the order of minutes or hours. When embedded in its ECM, the chondrocyte response is substantially different. Mechanical loading of the tissue leads to a fluid pressure difference between intracellular and extracellular compartments on the order of tens of kilopascals and the transmembrane outflow, on the order of a nanometer per second, subsides in about 1 h. The volume of the chondrocyte decreases concomitantly with that of the ECM. The interstitial fluid flow in the ECM is directed around the cell, with peak values on the order of tens of nanometers per second. The viscous fluid shear stress acting on the cell surface is several orders of magnitude smaller than the solid matrix shear stresses resulting from the ECM deformation. These results provide new insight toward our understanding of water transport in chondrocytes.

Acknowledgements This study was supported by funds from the National Institutes of Health (AR46532, EB004532).

References

- Almeida ES, Spilker RL (1997) Mixed and penalty finite element models for the nonlinear behavior of biphasic soft tissues in finite deformation: Part I – alternate formulations. *Comput Methods Biomech Biomed Eng* 1:25–46
- Andarawis NA, Seyhan SL, Mauck RL, Soltz MA, Ateshian GA, Hung CT (2001) A novel permeation device for hydrogels and soft tissues. In: *Proceedings of the 2001 ASME international mechanical engineering congress and exposition*, p 23149
- Armstrong CG, Lai WM, Mow VC (1984) An analysis of the unconfined compression of articular cartilage. *J Biomech Eng* 106:165–173
- Ateshian GA, Wang H (1995) A theoretical solution for the frictionless rolling contact of cylindrical biphasic articular cartilage layers. *J Biomech* 28:1341–1355
- Ateshian GA, Lai WM, Zhu WB, Mow VC (1994) An asymptotic solution for the contact of two biphasic cartilage layers. *J Biomech* 27:1347–1360
- Ateshian GA, Likhitanichkul M, Hung CT (2006) A mixture theory analysis for passive transport in osmotic loading of cells. *J Biomech* 39:464–475
- Bachrach NM, Valhmu WB, Stazzone E, Ratcliffe A, Lai WM, Mow VC (1995) Changes in proteoglycan synthesis of chondrocytes in articular cartilage are associated with the time-dependent changes in their mechanical environment. *J Biomech* 28:1561–1569
- Bachrach NM, Mow VC, Guilak F (1998) Incompressibility of the solid matrix of articular cartilage under high hydrostatic pressures. *J Biomech* 31:445–451
- Buschmann MD, Gluzband YA, Grodzinsky AJ, Kimura JH, Hunziker EB (1992) Chondrocytes in agarose culture synthesize a mechanically functional extracellular matrix. *J Orthop Res* 10:745–758
- Freeman PM, Natarajan RN, Kimura JH, Andriacchi TP (1994) Chondrocyte cells respond mechanically to compressive loads. *J Orthop Res* 12:311–320

- Guilak F (2000) The deformation behavior and viscoelastic properties of chondrocytes in articular cartilage. *Biorheology* 37:27–44
- Guilak F, Mow VC (2000) The mechanical environment of the chondrocyte: a biphasic finite element model of cell-matrix interactions in articular cartilage. *J Biomech* 33:1663–1673
- Guilak F, Ratcliffe A, Mow VC (1995) Chondrocyte deformation and local tissue strain in articular cartilage: a confocal microscopy study. *J Orthop Res* 13:410–421
- Guilak F, Jones WR, Ting-Beall HP, Lee GM (1999) The deformation behavior and mechanical properties of chondrocytes in articular cartilage. *Osteoarthritis Cartilage* 7:59–70
- Haider MA, Guilak F (2000) An axisymmetric boundary integral model for incompressible linear viscoelasticity: application to the micropipette aspiration contact problem. *J Biomech Eng* 122:236–244
- Hou JS, Holmes MH, Lai WM, Mow VC (1989) Boundary conditions at the cartilage-synovial fluid interface for joint lubrication and theoretical verifications. *J Biomech Eng* 111:78–87
- Hou JS, Mow VC, Lai WM, Holmes MH (1992) An analysis of the squeeze-film lubrication mechanism for articular cartilage. *J Biomech* 25:247–259
- Hung CT, Henshaw DR, Wang CC, Mauck RL, Raia F, Palmer G, Chao PH, Mow VC, Ratcliffe A, Valhmu WB (2000) Mitogen-activated protein kinase signaling in bovine articular chondrocytes in response to fluid flow does not require calcium mobilization. *J Biomech* 33:73–80
- Hung CT, Costa KD, Guo XE (2001) Apparent and transient mechanical properties of chondrocytes during osmotic loading using triphasic theory and AFM indentation. In: Summer bioengineering conference, Snowbird, UT, p 625–626
- Jones WR, Ting-Beall HP, Lee GM, Kelley SS, Hochmuth RM, Guilak F (1999) Alterations in the Young's modulus and volumetric properties of chondrocytes isolated from normal and osteoarthritic human cartilage. *J Biomech* 32:119–127
- Krishnan R, Park S, Eckstein F, Ateshian GA (2003) Inhomogeneous cartilage properties enhance superficial interstitial fluid support and frictional properties, but do not provide a homogeneous state of stress. *J Biomech Eng* 125:569–577
- Lee DA, Bader DL (1995) The development and characterization of an in vitro system to study strain-induced cell deformation in isolated chondrocytes. *In Vitro Cell Dev Biol Anim* 31:828–835
- Leipzig ND, Athanasiou KA (2005) Unconfined creep compression of chondrocytes. *J Biomech* 38:77–85
- Mansour JM, Mow VC (1976) The permeability of articular cartilage under compressive strain and at high pressures. *J Bone Joint Surg Am* 58:509–516
- Maroudas A (1979) Physicochemical properties of articular cartilage. In: Freeman MAR (ed) *Adult articular cartilage*, 2nd edn. Pitman Medical, Kent
- Maroudas A, Bullough P (1968) Permeability of articular cartilage. *Nature* 219:1260–1261
- Maroudas A, Ziv I, Weisman N, Venn M (1985) Studies of hydration and swelling pressure in normal and osteoarthritic cartilage. *Biorheology* 22:159–169
- Mauck RL, Soltz MA, Wang CC, Wong DD, Chao PH, Valhmu WB, Hung CT, Ateshian GA (2000) Functional tissue engineering of articular cartilage through dynamic loading of chondrocyte-seeded agarose gels. *J Biomech Eng* 122:252–260
- Mauck RL, Hung CT, Ateshian GA (2003) Modeling of neutral solute transport in a dynamically loaded porous permeable gel: implications for articular cartilage biosynthesis and tissue engineering. *J Biomech Eng* 125:602–614
- McGann LE, Stevenson M, Muldrew K, Schachar N (1988) Kinetics of osmotic water movement in chondrocytes isolated from articular cartilage and applications to cryopreservation. *J Orthop Res* 6:109–115
- Mow VC, Mansour JM (1977) The nonlinear interaction between cartilage deformation and interstitial fluid flow. *J Biomech* 10:31–39
- Mow VC, Kuei SC, Lai WM, Armstrong CG (1980) Biphasic creep and stress relaxation of articular cartilage in compression: theory and experiments. *J Biomech Eng* 102:73–84
- Mow VC, Gu WY, Chen FH (2005) Structure and function of articular cartilage and meniscus. In: Mow VC, Huiskes R (eds) *Basic orthopaedic biomechanics and mechano-biology*, 3rd edn. Lippincott Williams & Wilkins, Philadelphia
- O'Hara BP, Urban JP, Maroudas A (1990) Influence of cyclic loading on the nutrition of articular cartilage. *Ann Rheum Dis* 49:536–539
- Shieh AC, Athanasiou KA (2005) Biomechanics of single zonal chondrocytes. *J Biomech* DOI 10.1016/j.jbiomech.2005.05.002 (in press)
- Shin D, Athanasiou K (1999) Cytoindentation for obtaining cell biomechanical properties. *J Orthop Res* 17:880–890
- Smith RL, Trindade MC, Ikenoue T, Mohtai M, Das P, Carter DR, Goodman SB, Schurman DJ (2000) Effects of shear stress on articular chondrocyte metabolism. *Biorheology* 37:95–107
- Soltz MA, Ateshian GA (2000) A conewise linear elasticity mixture model for the analysis of tension-compression nonlinearity in articular cartilage. *J Biomech Eng* 122:576–586
- Spilker RL, Suh JK, Mow VC (1992) A finite element analysis of the indentation stress-relaxation response of linear biphasic articular cartilage. *J Biomech Eng* 114:191–201
- Stockwell RA, Barnett CH (1964) Changes in permeability of articular cartilage with age. *Nature* 201:835–836
- Trickey WR, Lee GM, Guilak F (2000) Viscoelastic properties of chondrocytes from normal and osteoarthritic human cartilage. *J Orthop Res* 18:891–898
- Trickey WR, Vail TP, Guilak F (2004) The role of the cytoskeleton in the viscoelastic properties of human articular chondrocytes. *J Orthop Res* 22:131–139
- Trickey WR, Baaijens FP, Laursen TA, Alexopoulos LG, Guilak F (2006) Determination of Poisson's ratio of the cell: recovery properties of chondrocytes after release from complete micropipette aspiration. *J Biomech* 39:78–87
- Wayne JS, Woo SL, Kwan MK (1991) Application of the u-p finite element method to the study of articular cartilage. *J Biomech Eng* 113:397–403
- Wilkes R, Athanasiou KA (1996) The intrinsic incompressibility of osteoblast-like cells. *Tissue Eng* 2:167–181
- Wu JZ, Herzog W (2000) Finite element simulation of location- and time-dependent mechanical behavior of chondrocytes in unconfined compression tests. *Ann Biomed Eng* 28:318–330
- Wu JZ, Herzog W, Epstein M (1999) Modelling of location- and time-dependent deformation of chondrocytes during cartilage loading. *J Biomech* 32:563–572
- Xu X, Cui Z, Urban JP (2003) Measurement of the chondrocyte membrane permeability to Me₂SO, glycerol and 1,2-propanediol. *Med Eng Phys* 25:573–579